Pulmonary toxicity of molybdenum disulphide after inhalation in mice

Sørli, Jorid B.; Jensen, Alexander C.Ø.; Mortensen, Alicja; Szarek, Józef; Gutierrez, Claudia A.T.; Givelet, Lucas; Loeschner, Katrin; Loizides, Charis; Biskos, George; More Authors

DOI
10.1016/j.tox.2023.153428

Publication date
2023

Document Version
Final published version

Published in
Toxicology

Toxicology 485 (2023) 153428

Contents lists available at ScienceDirect

Toxicology

journal homepage: www.elsevier.com/locate/toxicol

Pulmonary toxicity of molybdenum disulphide after inhalation in mice

Jorid B. Sørli [a,*], Alexander C.Ø. Jensen [a], Alicja Mortensen [a], Józef Szarek [b], Claudia A. T. Gutierrez [a,c], Lucas Givelet [d], Katrin Loeschner [d], Charis Loizides [e], Iosif Hafez [e], George Biskos [e,f], Ulla Vogel [a,g], Niels Hadrup [a,h,*]

[a] National Research Centre for the Working Environment (NFA), 105 Lersø Parkallé, Copenhagen Ø, Denmark
[b] Department of Pathophysiology, Forensic Veterinary Medicine and Administration, University of Warmia and Mazury in Olsztyn, Olsztyn, Poland
[c] Department of Public Health, University of Copenhagen, Copenhagen, Denmark
[d] Research Group for Analytical Food Chemistry, National Food Institute, Technical University of Denmark, DK-2800 Kgs, Lyngby, Denmark
[e] Climate and Atmosphere Research Centre, The Cyprus Institute, Nicosia 2121, Cyprus
[f] Faculty of Civil Engineering and Geosciences, Delft University of Technology, 2628 CN Delft, the Netherlands
[g] DTU Food, Technical University of Denmark, Kgs. Lyngby, Denmark
[h] Research group for Risk-Benefit, National Food Institute, Technical University of Denmark, Denmark

ARTICLE INFO

Keywords:
Comet assay
DNA damage
molybdenum disulfide
MoS2

ABSTRACT

Molybdenum disulphide (MoS_2) is a constituent of many products. To protect humans, it is important to know at what air concentrations it becomes toxic. For this, we tested MoS_2 particles by nose-only inhalation in mice. Exposures were set to 13, 50 and 150 mg MoS_2/m^3 (=8, 30 and 90 mg Mo/m^3), corresponding to Low, Mid and High exposure. The duration was 30 min/day, 5 days/week for 3 weeks. Molybdenum lung-deposition levels were estimated based on aerosol particle size distribution measurements, and empirically determined with inductively coupled plasma-mass spectrometry (ICP-MS). Toxicological endpoints were body weight gain, respiratory function, pulmonary inflammation, histopathology, and genotoxicity (comet assay). Acellular reactive oxygen species (ROS) production was also determined. The aerosolised MoS_2 powder had a mean aerodynamic diameter of 800 nm, and a specific surface area of 8.96 m^2/g. Alveolar deposition of MoS_2 in lung was estimated at 7, 27 and 79 μg/mouse and measured as 35, 101 and 171 μg/mouse for Low, Mid and High exposure, respectively. Body weight gain was lower than in controls at Mid and High exposure. The tidal volume was decreased with Low and Mid exposure on day 15. Increased genotoxicity was seen in bronchoalveolar lavage (BAL) fluid cells at Mid and High exposures. ROS production was substantially lower than for carbon black nanoparticles used as bench-mark, when normalised by mass. Yet if ROS of MoS_2 was normalised by surface area, it was similar to that of carbon black, suggesting that a ROS contribution to the observed genotoxicity cannot be ruled out. In conclusion, effects on body weight gain and genotoxicity indicated that Low exposure (13 mg MoS_2/m^3, corresponding to 0.8 mg/m^3 for an 8-hour working day) was a No Observed Adverse Effect Concentration (NOAEC,) while effects on respiratory function suggested this level as a Lowest Observed Adverse Effect Concentration (LOAEC).

1. Introduction

Molybdenum is an essential element required by enzymes that catalyse key reactions in the carbon, sulphur and nitrogen metabolism (Mendel and Bittner, 2006). Molybdenum disulphide (MoS_2) is a transition metal dichalcogenide. MoS_2 is a silvery black solid in its bulk form, is insoluble in water, and has many properties similar to graphite. MoS_2 powder has been used as dry lubricant for centuries (Winer, 1967), and is used in spray-formulated lubricants intended for machine parts (Sørli et al., 2022). Spraying such lubricants brings the substance into the aerosol state, which can be inhaled. To assess the impacts on human health from exposure to this substance, it is important to determine the concentration in ambient air at which it becomes toxic.

To the best of our knowledge, no peer-reviewed studies on the

* Correspondence to: National Research Centre for the Working Environment, Lersø Parkallé 105, DK-2100 Copenhagen Ø, Denmark.
E-mail addresses: jbs@nfa.dk (J.B. Sørli), alexander.co.jensen@gmail.com (A.C.Ø. Jensen), aam@nfa.dk (A. Mortensen), szarek@uwm.edu.pl, jozef.szarek@wp.pl (J. Szarek), xcag@nfa.dk (C.A.T. Gutierrez), lgiv@food.dtu.dk (L. Givelet), kals@food.dtu.dk (K. Loeschner), c.loizides@cyi.ac.cy (C. Loizides), i.hafez@cyi.ac.cy (I. Hafez), g.biskos@cyi.ac.cy (G. Biskos), ubv@nfa.dk (U. Vogel), nih@nfa.dk (N. Hadrup).

https://doi.org/10.1016/j.tox.2023.153428
Received 3 November 2022; Received in revised form 3 January 2023; Accepted 10 January 2023
Available online 11 January 2023

inhalation toxicity of MoS_2 exist to date. For other molybdenum-containing substances, one study by the National Toxicology Program (NTP) investigated 13-week inhalation of molybdenum-trioxide (MoO_3) in mice and rats. The rats were exposed to 1, 3, 10, 30, or 100 mg MoO_3/m^3 (=0.66–66 mg Mo/m^3), 6.5 h/day, 5 days/week. No changes were seen in clinical signs, body weight, organ weights, biochemistry, haematology or semen parameters. In addition, two-year (chronic) inhalation studies were conducted in both rats and mice, where chronic inflammation was seen in the lungs at 30 and 100 mg/m^3, while histopathological lesions were seen already at 10 mg/m^3. The evidence for carcinogenicity was equivocal in male rats; there was no evidence in female rats, whereas there was some evidence for carcinogenicity in mice (Chan, 1998; NTP, 1997). Hamsters inhaled MoO_3 nanoparticles at 5 mg/m^3 (=3.3 mg Mo/m^3) 4 h per day for 8 days. At 1 day post-exposure, neutrophils, and multinucleated macrophages were increased in the bronchoalveolar lavage (BAL) fluid. After 7 days, lymphocytes were increased in the same fluid (Huber and Cerreta, 2022). One caveat to take into account when comparing MoS_2 to MoO_3 is that the two substances have different physico-chemical properties that may affect their toxicological properties.

To our knowledge, there is no data on the in vivo genotoxicity or carcinogenicity of MoS_2 (Hadrup et al., 2022). One in vitro study reported no genotoxicity in human kidney epithelial cells (HEK293f) nor in *Salmonella typhimurium* (Appel et al., 2016). Concerning other molybdenum substances, molybdenum nanoparticles were genotoxic in vivo (Mohamed et al., 2020). Molybdenum (IV) sulphide nano- and microparticles were not genotoxic in vivo (Sobańska et al., 2020), while there were both a positive and a negative in vivo study on sodium molybdate (ECHA, 2020; Titenko-Holland et al., 1998). Several molybdenum substances tested in vitro showed no genotoxicity, while only a few did (Hadrup et al., 2022).

Overall, we found no reports in the literature on the inhalation toxicity of MoS_2. Thus, we set out to determine air concentrations at which this substance exerts toxicity. As model organism, we used male mice. The exposure was achieved through inhalation of MoS_2 particles having an aerosolised aerodynamic size of 800 nm. The exposure levels were 13, 50 and 150 mg/m^3 (= 8, 30 and 90 mg Mo/m^3), designated Low, Mid and High exposure. The duration was 30 min/day, 5 days per week for 3 weeks. The duration was limited to 30 min per day for animal ethical reasons. For particle toxicity, the daily dose can be calculated as concentration multiplied by exposure duration (Haber's rule) (Brand et al., 2014). Endpoints were clinical appearance, body weight gain, respiratory function, pulmonary inflammation, histopathology, and genotoxicity assessed by the comet assay. The specific surface area, and acellular reactive oxygen species (ROS) production were determined for the MoS_2 powder. Molybdenum levels were determined in the lungs using inductive coupled plasma – mass spectrometry (ICP-MS).

2. Methods

2.1. MoS_2 properties

We used a commercially available MoS_2 powder (CAS number: 1317–33–5) (Molybdenum(IV)Sulfide, MoS_2, MW: 160.1 g/mol) with grain sizes reported by the manufacturer to be < 2 μm, and a reported purity of 99% (Sigma-Aldrich, Prod. No. 234842).

The surface area of the powders was analysed by nitrogen absorption Brunauer–Emmett–Teller (BET) theory analysis (3 P sync 110). In brief, samples were dried at 200ºC under vacuum for 2 h, weighed (with amounts ranging from 14 to 130 mg) and analysed with the static volumetric method using N_2 as the adsorbate.

The MoS_2 powder was aerosolised using a venturi-type rotating disc microfeeder (Fraunhofer Institute für Toxicologie und Aerosolforschung, Hannover, Germany), at a pre-pressure of 5 bar. The particle laden airstream was directed through an aerosol mixing and sedimentation glass-tube to the exposure chamber with a total volume-flow rate of 20 L/min. Mass-concentrations of total suspended powder mass were evaluated gravimetrically by filter sampling to calculate the resulting average concentration levels of 13 (Low exposure), 50 (Mid exposure) or 150 mg/m^3 (High exposure) in the chamber. Chamber air was sampled during each exposure on Millipore Fluoropore filters (∅ 2.5 cm; pore size 0.45 μm) at an airflow of 2 L/min, using Millipore cassettes for a duration of 30 min for control, 15 min for Low exposure, and 5 min for Mid and High exposure. Acclimatised filters were pre-weighed on a Sartorius Microscale (Type M3P 000 V001). Final gravimetric data were obtained on filters acclimatised (50% RH and 20 °C) for at least 24 h (level of detection was: 0.003 mg/filter). Particle number and aerodynamic particle size distributions resulting from the aerosolisation method were measured in 14 size channels between 6 nm and 10 μm with 1-second intervals using an Electrical Low Pressure Impactor (ELPI+, Dekati Ltd., Tampere, Finland). Control animals were exposed to HEPA filtered air through a clean venturi-type tube to generate the same level of noise as for the MoS_2 exposed animals.

The estimated alveolar deposition was determined based on an estimated pulmonary deposited mass rate calculated with the Multiple-Path Particle Dosimetry Model (MPPD) (version 3.04, ARA, Huntsville, AL United States), using the exposure levels (13, 50 and 150 mg/m^3), exposure time (30 min over15 days). MMAD and GSD were calculated based on the mode of the aerosol (Supplemental Fig. S1). Input parameters in the MPPD model are detailed in the Supplemental Materials.

2.2. Animal procedures

The experiments were carried out in accordance with the Danish Animal Experimentation Act (LBK nr 474 of 15/05/2014 and BEK nr 12 of 07/01/2016) and the EU-directive 2010/63/EU on the protection of animals used for scientific purposes. Permission for the study was obtained from by the Animal Experimentation Inspectorate, Ministry of Food, Agriculture and Fisheries of Denmark (License No. 2019–15–0201–00114). Male BALBC/J mice, 6–7 weeks of age, were obtained from Janvier (France). In total 36 mice were purchased covering four in the pilot, and 32 in the main study. Upon arrival, the animals were randomised to cages with either control or MoS_2 administered animals (n = 2 animals per cage, and n = 8 per treatment group). The animals had ad libitum access to drinking water (tap water) and feed (Altromin no. 1324, Brogaarden, Denmark). The mice were housed in 1290D Eurostandard Type 3 polypropylene cages with Enviro-Dri bedding (Brogaarden, Gentofte, Denmark). Wood blocks served as enrichment (Brogaarden, Gentofte, Denmark). Room temperature and humidity were kept within 20 ± 2 °C and 50 ± 20%, respectively. The animals were housed under a 12 h light/12 h dark cycle (light on from 6 a.m.). The animals had one week of acclimatisation and one week of training in the plethysmograph tubes prior to the investigation. Training was done on five consecutive days, for 30 min each day. The inhalation was done nose-only with the animals placed in tubes inserted into the inhalation chamber.

A pilot study was carried out with a concentration of 150 mg MoS_2/m^3. First, one mouse was exposed to MoS_2 for 30 min over four consecutive days. On the 3rd day of exposure, three additional mice were also exposed, but these were only exposed twice. After exposure on day 4, all mice were killed by cervical dislocation and necropsied. There were no visible changes to the organs or weight loss. Based on the pilot study we decided to use 10, 50 and 150 mg/m^3 in the main study.

In the main study, mice were exposed in total 15 times for 30 min, with one daily exposure on all weekdays over a three-week period (in total 7.5 h). The total time in the exposure tubes was 45 min including baseline measurements, set-up period, and exposure period. Control animals were placed in the chamber with the same airflow of filtered air into the chamber, and the same amount of noise. In order to monitor toxicological effects occurring at the lowest exposure during the experiment, we used a staggered start in which Low exposure (10 mg/m^3) as well as 5 control animals were initiated during the first week, the

middle concentration one week later, and the highest concentration as well as 3 control animals one additional week later.

At the end of the experiment, the animals were anesthetised by subcutaneous injection of a combination of Zoletil 100 (zolazepam 250 mg/mL and tiletamine 250 mg/mL), Xysol (xylazine 20 mg/mL) and Fentadon (fentanyl 50 μg/mL) in sterile saline, at a volume of 0.1 mL/10 g bw, before they were killed by cardiac puncture. Thereafter BAL fluid was recovered and the animals underwent a detailed necropsy: external surface, all orifices, and thoracic, abdominal and pelvic cavities including viscera were inspected. Lung, liver and kidney were excised for further analysis and stored at − 80 °C.

2.3. Molybdenum concentration in lungs by ICP-MS

The frozen right lungs (weight between 160 mg and 260 mg, not comparable to normal lung weight as the lungs had been flushed with liquid to extract the BAL cells) were weighted in 18 mL quartz vials using an analytical Sartorius GENIUS ME balance (Göttingen, Germany) and 0.5 mL concentrated nitric acid (67–69% HNO_3, PlasmaPure, SCP Science, Quebec, Canada) and 0.1 mL ultrapure water (resistivity 18.2 mΩ·cm at 21.5 °C, Millipore Element apparatus, Millipore, Milford, MA, USA) added. The samples were digested in a microwave reaction system (Multiwave 7000, Anton Paar GmbH, Graz, Austria), using the following digestion program: ramp to T = 250 °C for 20 min, held at T = 250 °C for 10 min, cooled down for 30 min; the starting pressure was 40 bar and the maximum pressure 120 bar. After digestion, the samples were transferred to 15 mL disposable polypropylene tubes (Sarstedt AG & Co. KG, Germany), diluted with ultrapure water to a final sample volume of approximately 10 mL, weighted and the density determined. Prior to ICP-MS analysis, the digested samples were further diluted two-fold with 2% HNO_3. For quality assurance, blank samples (N = 6) and the reference material SRM 1577c Bovine liver (NIST, MA, USA) with a certified Mo concentration of 3.30 ± 0.13 mg/kg (N = 6) were included in all analyses. For digestion of the reference material, we used approximately 0.3 g of the sample (dry mass).

The total mass concentration of Mo in the digested samples was determined using an iCAP TQ ICP-MS (Thermo Fisher Scientific, Bremen, Germany) equipped with an ASX-560 autosampler (Teledyne CETAC Technologies, Omaha, NE, USA). The analysis was performed in single quadrupole mode without any cell gas. Determination of the Mo mass concentrations was performed based on external calibration by measuring Mo standards in the concentration range from 0 to 40 μg/L with internal standardisation (1 μg/L rhodium (Rh). Calibration and internal standards were prepared from standard solutions that contained 1000 mg/L of Mo or Rh (PlasmaCAL, SCP Science, Baie D'Urfé, QC, Canada). All standards were matrix-matched with the diluted samples (i.e., prepared in 2% HNO_3). Instrumental configuration and operating parameters for ICP-MS analysis are provided in Supplemental Materials Table S1.

The limit of detection (LOD) and limit of quantification (LOQ), calculated as 3- and 10-times standard deviation of the blank samples and considering the sample dilution, were 1 and 4 ng/g, respectively. The average mass concentration of Mo determined in the blank samples was subtracted from the Mo mass concentrations determined in the corresponding mouse samples. The average recovery based on the certified reference material was found to be satisfactory from 80% and 120%. The repeatability was satisfactory with a relative standard deviation less than 2%. The total amount of molybdenum in the right lung was multiplied by 1.75 to obtain the amount in the whole lung. This factor is based on differences in the weight of the right and left side of the lung in previous measurements of 17 C57BL/6 J mice, 20–24 g in body weight (the weight of the right lung constituted 57% of the whole lung).

2.4. Lung function measurements using a plethysmograph

We measured the animals' respiration in a plethysmograph both in the pilot study (all exposure days) and in the main study on days 1, 9 and 15 (Nielsen et al., 2005). The following days and exposures have data for respiration: Low exposure and five controls; days 1, 9 and 15, Mid exposure; days 1 and 15, High exposure and three controls; days 1 and 9 (data not available on all days due to absence of staff). On these days, the animals were placed in the plethysmograph tubes while on the other days of exposure the animals were placed in head-out-only tubes, in which they could move their head freely. The animals were trained in the plethysmograph tubes for one week prior to the investigation on 5 consecutive days, 30 min on each day. The position of the head of the mice in the exposure chamber was the same both when exposure in the plethysmograph tube, and the head- only tubes were done (Vijayaraghavan et al., 1993). Respiratory parameters were collected using Notocord Hem (Notocord Systems SA, Croissy-sur-Seine, France). Prior to exposure, a 15-minute baseline period was recorded for each mouse. If the mouse did not adjust to the plethysmograph tube during the baseline measurement, it was transferred to a regular exposure tube prior to exposure. To assess exposure-related effects, the respiratory parameters during exposure were compared to baseline levels for each mouse. Several breathing parameters were analysed including respiratory frequency, tidal volume, time of break, which is the period after inspiration before expiration (prolongation is a sign of upper respiratory tract irritation) and time of pause, which is the period after expiration before the next inspiration (prolongation is a sign of pulmonary irritation) (Nielsen et al., 2005; Vijayaraghavan et al., 1994).

2.5. BAL fluid cellularity and biochemistry

BAL fluid was obtained just after the animals had been killed, by flushing the whole lungs with saline and BAL fluid cellularity was measured as previously reported (Kyjovska et al., 2015). Lactate dehydrogenase (LDH) was assessed in BAL fluid with an ELISA kit from Abcam (Product number: 02526) according to the manufacturer's protocol; while protein was measured with a Pierce BCA Protein Assay Kit from Thermo Scientific (Product number 23227) according to the manufacturer's protocol.

2.6. Histopathology

Livers and kidneys were fixed in 4% neutral buffered formaldehyde solution for at least 24 h, thereafter trimmed, dehydrated and embedded in paraffin. Sections 2–2.5 μm in thickness were cut on a microtome and stained with the haematoxylin and eosin (H&E) stain (Histolab Products AB, Askim, Sweden). Histological examination by light microscopy in brightfield mode was performed on all samples from the control and High exposure groups by two operators at first with knowledge of treatment groups and thereafter blindly (Haschek et al., 2010). The INHAND proposal for diagnostic nomenclature of microscopic changes in rodents was followed (Frazier et al., 2012; Thoolen et al., 2010). When present, inflammatory cell infiltrates (focal infiltrations of mono- and poly-nuclear and/or histiocytic cells) in the liver were classified into two categories: small (< 10 inflammatory cells, sporadically accompanied by necrotic hepatocytes with distinct eosinophilic cytoplasms) and big (> 10 inflammatory cells typically surrounded by necrotic hepatocytes with distinct eosinophilic cytoplasm and with apoptotic bodies/debris often present) and their numbers were recorded. The severity scores were given for the following changes in the livers: cytoplasmic vacuolation of hepatocytes (hydropic degeneration), apparent increase in Kupffer cells, apparent increase in binucleate hepatocytes, congestion and extravasation, and for vacuolation of tubular epithelial cells in the kidneys (Di Ianni et al., 2020; Modrzynska et al., 2021). The severity was evaluated using a 4-grade scoring system: grade 1: minimal/very few/very small; grade 2: mild/few/small; grade 3: moderate/moderate

number/moderate size; grade 4: marked/many/large. For other changes, the presence was recorded and incidence for each group reported.

As part of the differential counting procedure we also observed whether the cells showed abnormal morphology.

2.7. Genotoxicity measured with comet assay

The level of DNA strand breaks was assessed in BAL cells, and lung (left lung) and liver tissue as tail percent DNA, measured by the comet assay using the IMSTAR PathFinder system as described previously (Hadrup et al., 2017; Jackson et al., 2013). In brief, after collection, the BAL fluid was immediately placed on ice until isolation of the cells by centrifugation at 400 g for 10 min at 4 °C. The cells were then resuspended in 100 μL of HAM's F12 medium (with 1%penicillin-streptomycin, 1% L-glutamine and 10% foetal bovine serum (FBS)). Then 40 μL of the resuspension was mixed with 60 μL of freezing medium (HAM's F12 medium with 1% penicillin-streptomycin, 1% L-glutamine, 10% FBS and 10% dimethyl sulphoxide (DMSO)) and frozen at − 20 °C before storage at − 80 °C until comet analysis. Lung and liver samples were excised from the animals and ~20–40 mg of sample was cut (3 ×3 ×3 mm), transferred to NUNC cryotubes, frozen in liquid N_2 and stored at − 80 °C until comet analysis.

All samples were run in the comet assay on the same day. BAL cells kept in freezing medium were thawed at 37 °C, immediately embedded in 0.7% agarose, and placed on ice until loading onto a Trevigen Comet Slide (Trevigen, Gaithersburg, MD, USA). Lung and liver samples were in frozen condition pressed through a stainless steel cylindrical sieve (diameter 0.5 cm, mesh size 0.4 mm) into 0.5–2 mL ice-cold Merchant's medium (0.14 M NaCl, 1.47 mM KH_2PO_4, 2.7 mM KCl, 8.1 mM Na_2HPO_4, 10 mM Na_2EDTA, pH 7.4) and placed on ice before being embedded in 0.7% agarose and loaded onto a Trevigen Comet Slide. The slide was incubated overnight with 4 °C cold lysing buffer (2.5 M NaCl, 10 mM Tris, 100 mM sodium-ethylenediaminetetraacetic acid (EDTA), 1% sodium sarcosinate, 10% DMSO, 1% Triton X-100, pH 10). Next, the slide was rinsed for 5 min in cold electrophoresis buffer, and then transferred to the electrophoresis chamber where it was alkaline treated with ice-cold electrophoresis buffer (0.3 M NaOH, 1 mM sodium-EDTA, pH 13.2) for 35 min. The electrophoresis was run for 25 min at 38 V (1.2 V/cm) and then the slide was rinsed in neutralisation buffer (0.4 M Tris, pH 7.5) two times 5 min, and fixed for 5 min in 96% ethanol followed by 15 min at 45 °C. The cell nuclei were stained with SYBR® Green in TE buffer (10 mM Tris–HCl, 1 mM EDTA, pH 7.6). Scoring was done automatically in the IMSTAR PathFinder system. Percentage DNA in the comet tail was evaluated as the measure of DNA strand breaks. Very long tails indicative of apoptosis were visually inspected for. Negative and positive controls were included on all slides these were A549 cells exposed to 0 or 45 μM of H_2O_2, respectively.

2.8. Reactive oxygen species (ROS) production of the MoS2 powder

The generation of reactive oxygen species (ROS) by MoS2 was measured using the 2′− 7′-dichlorodihydro-fluorescein diacetate ($DCFH_2$-DA) oxidation assay, as described previously (Bengtson et al., 2016; Danielsen et al., 2020). Briefly, a particle stock suspension of 1.35 mg MoS_2/mL was prepared with Hank's balanced salt solution (HBSS), and sonicated with an amplitude of 10% on ice for 16 min using an S-450D Branson Sonifier (Branson Ultrasonics Corp., USA). The apparatus delivers 7.3 Watts at this amplitude (Booth and Jensen, 2015). Dilutions from the stock suspension were prepared in HBSS (0, 1.1, 2.1, 4.2, 8.4, 16.9, 33.8, 67.5 and 101.3 μg MoS_2/mL). $DCFH_2$-DA was deacetylated to $DCFH_2$ with 0.01 M NaOH, for 30 min at room temperature, and diluted with HBSS. Particle dilutions were added in triplicates to a 96-well plate, followed by $DCFH_2$. Finally, plates were incubated for 3 h at 37 °C, and fluorescence of the formed 2′− 7′-dichlorofluorescein (DCF) was measured with an excitation wavelength of 490 nm and emission wavelength of 520 nm, using a 1420 Victor^2 multilabel counter (Perkin Elmer, Denmark). In the present study, Printex 90 was used as reference material due to its high ROS production (Boyles et al., 2022; Jacobsen et al., 2008). To evaluate the MoS_2 potential of producing ROS, we performed a linear regression and used the slopes from the linear range of the concentration-response curves: 0–16.9 μg/mL for Printex 90 and 0–33.8 μg/mL for MoS_2.

2.9. Statistics

We employed the Graph Pad Prism software package 7.02 (Graph Pad Software Inc., La Jolla, CA, USA) for all the statistical analyses carried out in this work. First data were tested for normality with the Shapiro-Wilk test. The parametric ANOVA test is relatively robust against deviations from normality, but somewhat sensitive to differences in standard deviation. Hence this test was calculated, except if the P value of the Shapiro-Wilk test was very low ($P < 0.001$), or if standard deviations were very different in the Brown-Forsythe tests ($P < 0.001$). In case data had the described deviations in normality or standard deviations, we planned to calculate the non-parametric Kruskall-Wallis test. Holm-Sidak's multiple comparisons test (ANOVA) and Dunn's multiple comparisons test (Kruskall-Wallis test) were applied, respectively, to assess differences in between control and dosage groups in the one-way ANOVA or Kruskall-Wallis test. For the plethysmograph data, we did a two-way ANOVA with repeated measurements to test for differences between controls, and treated animals over the time period of the measurements. In case of missing values, Graph Pad Prism was set to automatically switch to a Mixed-effects model (REML).

3. Results

3.1. MoS_2 specific surface area and size distribution

BET analysis showed that the specific surface area of our sample particles is 8.96 m^2/g. The total pore volume (at p/p0 = 0.99000) was 0.038 cm^3 /g; the average pore diameter (4 V/A) was 17.2 nm. Moreover, HK/SF micropore analysis (< 2 nm) gave a micropore volume of 0.004 cm^3 /g; a most frequent pore diameter of 0.849 nm; and a median pore diameter of 0.92 nm.

The median number aerodynamic diameter mode of the aerosolised MoS_2 was determined from the measured number size distribution and was found to be 800 nm (Supplemental Materials Fig. S1) (Mass mean aerodynamic diameter (MMAD): 2.75 μm, GSD: 1.9). This is in the respirable range of BALB/c mice (<1 μm) (Asgharian et al., 2014), with the note that the upper part of the spectrum is somewhat higher than the respirable range (Supplemental Materials Fig. S1). The particle size-distribution was found to be consistent over all concentrations and generation rates. The chamber mass concentrations measured on the filters were determined to be 13 ± 5 (mean±SD), 50 ± 11 and 150 ± 42 mg MoS_2/m^3, for Low, Mid and High exposure, respectively.

3.2. Body weight and clinical appearance

3.2.1. Pilot study

The animals exhibited no clinical signs of toxicity during the study. One mouse exposed to 150 mg MoS_2/m^3 for four times 30 min lost 6% of body weight, which stabilised to 2% at the end of the pilot experiment. The three other animals had a body weight increase of 0–3% from onset to end (after 2 days of exposure). Respiratory function was measured during all exposures and no effect was seen.

3.2.2. Main study

The main study was based on the pilot study data conducted with exposures of 13, 50 and 150 mg MoS_2/m^3. The animals exhibited no clinical signs of toxicity during the study. The end body weight was not different among the groups (data not shown). It is important to note that

as we had a staggered start, the Mid and High exposure animals, and half of the controls were older during exposure than the Low exposure animals and the remaining controls. Therefore, body weight gain is a better measure of body weight changes over the study. There is a clear decrease in body weight gain at High exposure ($P < 0.001$) and a decrease with borderline statistical significance in Mid exposure ($P = 0.04$), as compared to control. At Low exposure, the body weight gain was not different from control (Fig. 1).

3.3. Level of alveolar deposition of molybdenum in lungs

The MoS_2 particle lung-deposition was both calculated based on the aerosolised particle distribution, and determined empirically by ICP-MS. Alveolar deposition of MoS_2 in lung was with the MPPD model estimated to be 7, 27 and 79 μg MoS_2/mouse based on the aerosolised particle size distribution (Table 1). By ICP-MS the deposition was determined to be 21, 60 and 103 μg Mo/mouse, which corresponds to 35, 101 and 171 μg MoS_2/mouse for Low, Mid and High exposure, respectively (Fig. 2 and Table 1) assuming that all Mo is present as MoS_2.

3.4. Respiratory function

On day 15, there was a decrease in tidal volume for both Low and Mid exposure (the endpoint was not assessed for High exposure due to unexpected absence of staff). This decrease in tidal volume was seen in absence of compensatory increases in breathing frequency (Fig. 3). The same pattern was seen at day 1 for Low exposure, while no effects were seen in either of these endpoints at Mid and High exposure on day 1, nor at Low or High exposure on day 9 (Mid exposure not evaluated at day 9) (Supplemental Materials Fig. S2).

Concerning time of pause (the period before inspiration) and time of break (the period before expiration), the latter was increased at all three exposure levels on day 1 (indicating upper respiratory tract irritation). Such changes were not statistically different at other time points, however, we note that single animals in the Mid exposure group on day 15, and the High exposure group on day 9, had increased time of break (Supplemental Materials Fig. S3). No effects were seen on time of pause at any exposure level, indicating no irritation on the alveolar level (pulmonary irritation) (Supplemental Materials Fig. S3).

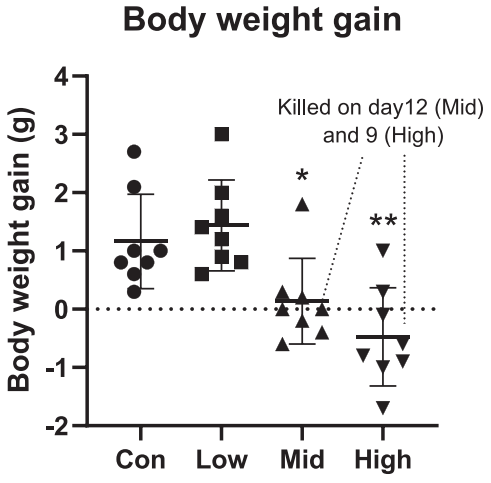

Fig. 1. Body weight gain. Con designates control mice exposed to filtered air. The horizontal lines show mean levels and the bars show SD. * * and * designate P values of < 0.01 and < 0.05, respectively, of one-way ANOVA with Holm-Sidak's multiple comparisons test. One animal in the Mid exposure group and one in the High exposure group were killed on day 12 and 9, respectively (before planned), to monitor for red spots on the lung seen at Low exposure.

3.5. Pulmonary inflammation measured as increased neutrophils, other BAL fluid cells, and BAL fluid biochemistry

Lung inflammation, measured as increased neutrophil numbers in BAL fluid, was seen only for High exposure (Fig. 4). No effect was seen on macrophage numbers expressed as the total number of macrophages in the BAL fluid (the percentage of macrophages was decreased at High dose (Supplemental Materials Fig. S5), but morphologically the macrophages were abnormal at Low exposure having an appearance with what can be described as having foam inside. Particles were observed both inside macrophages and in the BAL fluid in all MoS_2 exposure groups, but not in the controls (data not shown). Other cell types including lymphocytes, eosinophils, and epithelial cells in BAL fluid were unaltered in terms of cell numbers (Supplemental materials Fig. S4). Total cells were only increased at High exposure, likely reflecting the increase in neutrophils. There were no differences in LDH or protein level in BAL fluid at any of the exposure levels (data not shown).

3.6. Histopathology

During the necropsy, we observed that the Low exposure mice had red spots on the lung, which resembled bleedings. Because of this, one Mid exposure and one High exposure animal were killed and examined on day 12 and 9, respectively. The two mice had no red spots on the lung. Moreover, on the planned termination day, none of the remaining Mid and High exposure animals had this phenomenon. No other macroscopic changes were found at necropsy. Histological examination of the livers and kidneys from the High exposure animals did not reveal any differences to the controls. The histological findings were of low incidence and minimal severity in both control and the High exposure animals (Supplemental materials Table S2 and S3). Some changes belonged either to a background morphology (e.g. large nuclei of hepatocytes, binucleate hepatocytes, mitosis) or to incidental findings (e.g. focal inflammatory cell aggregates or focal necrosis in the liver, vacuolated tubule cells in the renal cortex) (Harada et al., 1999; Seely, 1999). Congestion and extravasation were attributed to the bleeding technique in the absence of any histopathological correlates, with similar incidence and minimal severity in both control and High exposure.

3.7. Genotoxicity

Increased genotoxicity observed as percentage of DNA in the tail of BAL fluid cells was seen at Mid and High exposure (Fig. 4). No increase in DNA strand break levels was seen in lung and liver tissue (Supplementary Materials Fig. S6).

We found concentrations-dependent ROS production for MoS_2. On a mass basis, the ROS potential of the MoS_2 particles was lower than that observed with Printex 90 carbon black nanoparticles, as the slope obtained from MoS_2 was 6% of the slope of Printex 90 (MoS_2: 197 vs. carbon black: 3448 arbitrary units/μg/mL (Fig. 5). However, if ROS was normalised to surface area, (9 m^2/g for MoS_2 and ~300 for carbon black Printex 90), its potential was similar for the MoS_2 and carbon black particles (slope MoS_2: 2453 arbitrary units/cm^2/mL vs. 1168 for carbon black) (Supplemental Fig. S7).

4. Discussion

4.1. Clinical appearance and body weight

The body weight gain was lower for Mid and High exposure as compared with controls, albeit the effect at Mid exposure showed only borderline statistical significance ($P = 0.04$). To the best of our knowledge, there are no data in the peer-reviewed scientific literature reporting on body weight after inhalation of MoS_2. Thus, we have no previous data to compare with. The changes in body weight suggest a No Observed Adverse Effect Concentration (NOAEC) of 13 mg MoS_2/m^3

Table 1
Retained molybdenum and MoS_2, retained surface area, and estimated alveolar deposited dose in the lungs.

	Average Mo concentration (by ICP-MS) (μg/g) in BAL fluid flushed right lung	Standard deviation (μg/g)	Mo per whole lung (by ICP-MS) (μg)	MoS_2 per whole lung based on ICP-MS measurements of Mo (μg)	Retained surface area of MoS_2 (cm^2) calculated based on the ICP-MS data	Estimated alveolar deposited dose of MoS_2 (μg) at 15 days of exposure, using the MPPD model
Control	0.06	0.01	0.02	0.04	0	0
Low	58	7	21	35	3.1	7.0
Mid	168	25	60	101	9.0	27
High	271	36	103	171	15.4	79

The amount of Mo was determined by ICP-MS in the whole right lung and this number was converted to whole lung by multiplication with a factor of 1.75 as described in the Methods section. The retained surface area was calculated based on the ICP-MS data using a specific surface area of 0.0896 cm2/μg MoS2.

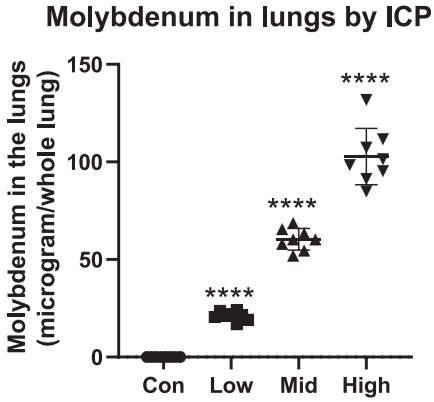

Fig. 2. Molybdenum concentration in the lungs determined by ICP-MS. Con designates control mice exposed to filtered air. The horizontal lines show mean levels and the bars show SD. * ** * designates a P value of < 0.0001, of one-way ANOVA with Holm-Sidak's multiple comparisons test.

based on this endpoint.

4.2. Respiratory effects

We observed a decreased tidal volume with MoS_2 inhalation at both Low and Mid exposure on day 15. It is unknown whether this effect would also have occurred at High exposure as we were not able to evaluate this endpoint on that day due to an unexpected absence of staff. A decreased tidal volume was also seen at Low exposure on day 1, while no decrease in tidal volumes was seen at the other exposure levels on this day, nor at any exposure level on day 9. That the effect seemed only to be profound on day 15, suggests that in the end of the 15-day period a change in the airways induced this effect. We did not assess the lungs for pathological changes, thus it is unknown if this change in breathing pattern manifests as changes in the tissues. This effect occurred in the absence of an increase in breaths per minute, thus the animals did not compensate for the decrease in tidal volume by increasing the breathing rate. Overall, the findings in this endpoint suggests effects on respiratory function already at Low exposure, one could argue that a decrease in tidal volume is an adverse effect as it may decrease the body's ability to compensate for additional stress that affects this endpoint (IPCS, 2004). Thus if we consider this effect adverse, then the Low dose could be suggested as a Lowest Observed Adverse Effect Concentration (LOAEC) of 13 mg MoS_2/m^3.

There was increased time of break (period between inspiration and expiration) on day 1 at all three exposure levels, suggesting an irritative effect in the upper airways (Nielsen et al., 2005; Vijayaraghavan et al., 1994). On days 9 and 15, increased time of break was found for individual animals only (not statistically significant on a group basis). This pattern implies that tolerance to irritation had developed over the study period. We found no increases in the time of pause, indicating that MoS_2 did not cause irritation at the alveolar level (pulmonary irritation).

Reviewing the literature on the pulmonary toxicity of molybdenum, we found only one study reporting effects on respiratory function, and this was for MoO_3. In that study, Ott and colleagues investigated 43 workers exposed to MoO_3 at a metal processing plant. Respiratory symptoms were reported for 33 of the workers, and exposed workers had a higher forced expired volume in the first second (FEV_1-%) and a higher forced vital capacity (FVC-%) than controls (Ott et al., 2004). Thus, these workers did not exhibit toxicity in terms of respiratory function – rather the contrary. One case study, published as a conference abstract, described acute toxicity with nausea, dyspnoea and circulatory shock, eventually resulting in death. The subject was a 69-year-old man who had treated the underbody of a car with a lubricant/penetrating oil. He had also exposed himself to aerosols of a rust remover spray containing MoS_2, petrol hydrocarbons, and carbon dioxide (propellant). During that treatment, he was laying under the car for approximately 15 min (Hahn et al., 2012).

4.3. Inflammation, pathology and alveolar deposition of molybdenum

We saw inflammation in the form of an increased neutrophil number at High exposure, suggesting Mid exposure as a NOAEC of 50 mg MoS_2/m^3. This was for a daily 30 min exposure, and this corresponds to 3.1 mg/m^3 for an 8-hour working day. We identified no peer-reviewed studies on the inhalation toxicity of MoS_2 reporting neutrophil numbers in BAL fluid. Notably, as inflammation is predicted by the total surface area of the retained particles in the lung, the primary particle size is an important determinant of inflammation (Cosnier et al., 2021). Concerning other molybdenum substances: in the aforementioned 43 workers exposed to MoO_3, increased neutrophil and lymphocyte numbers were seen in BAL fluid of symptomatic individuals (Ott et al., 2004). Another study described above investigated MoO_3 in a two-year (chronic) inhalation study with rats and mice. Chronic inflammation was seen in the lungs of both species at 20 and 66 mg Mo/m^3, while histopathological lesions were seen already at 6.6 mg Mo/m^3 ($NOAEC_{chronic\ inflammation\ in\ lungs}$: 5 mg Mo/$m^3$, LOAEC: 15 mg Mo/$m^3$, when adjusted to an 8-hour work day) (Chan, 1998; NTP, 1997). Finally, hamsters inhaled MoO_3 nanoparticles at 5 mg/m^3 for 4 h per day for eight days. One day later, neutrophils, and multinucleated macrophages were increased in BAL fluid ($LOAEC_{increased\ neutrophils}$: 4 mg Mo/$m^3$ or 2 mg/m^3 normalised to an 8-hour working day) (Huber and Cerreta, 2022). Thus, our data with a NOAEC of 50 mg MoS_2/m^3 corresponding to 3.1 mg/m^3 for an 8-hour working day are in line with the dose descriptors seen with other forms of molybdenum when exposures are normalised to working days.

We observed abnormal (foamy) macrophages in BAL fluid at Low exposure only. An explanation for this non-monotonous dose-response is that neutrophils take over at higher exposure levels to remove larger quantities of foreign material.

We previously found that the presence of copper in silica particles exerted a stronger inflammatory response than what would have been expected from the particle surface area (Hadrup et al., 2021), suggesting that released ions or the dissolution process may contribute to the inflammation of a metal-material. Yet in the current study, we cannot determine if our inflammation results are due to the particle form or released ions. Though notably, one study found that a MoS_2 powder

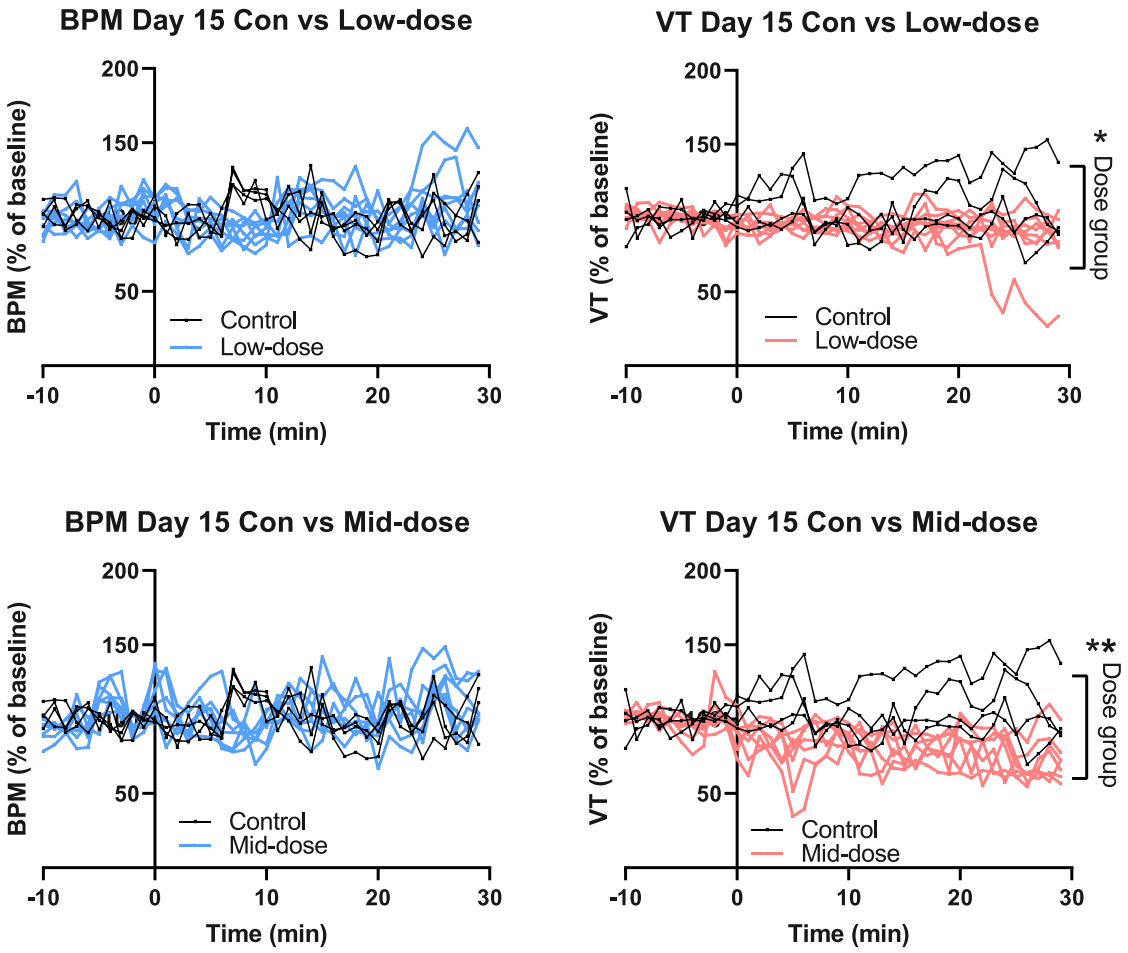

Fig. 3. Breathing frequency (breaths per minute, BPM) and changes in tidal volume (VT) at the last exposure day to MoS_2. Con designates control mice exposed to filtered air. The lines illustrate individual animals and the dots represent the mean during one minute of respiration. * * and * designate P values of < 0.01 or < 0.05, respectively, of exposure-group differences by two-way ANOVA; or in case of missing values, mixed-effects model (REML) for VT Day 15 Con vs Mid exposure and BPM Day 15 Con vs Mid exposure. High exposure was not assessed on day 15.

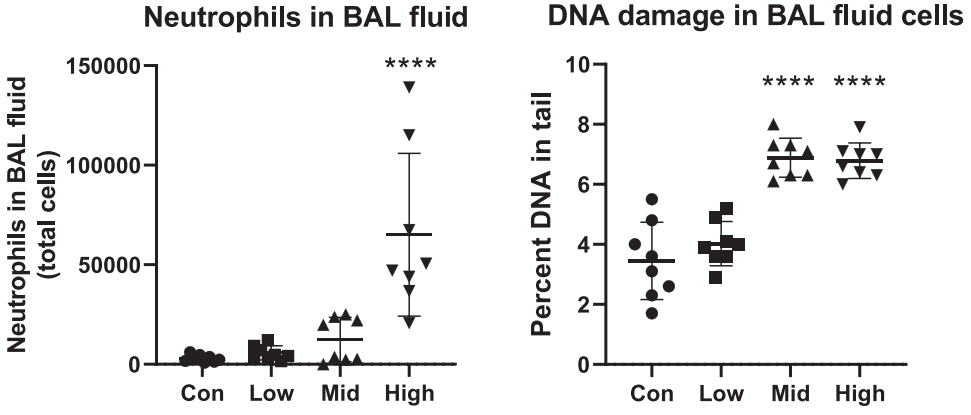

Fig. 4. Neutrophil numbers in bronchoalveolar lavage fluid and genotoxicity in BAL fluid cells of mice exposed to MoS_2 particles. Con designates control mice exposed to filtered air. The horizontal lines show mean levels and the bars show SD. * ** * designates P values of < 0.001 of one way ANOVA with Holm-Sidak's multiple comparisons test compared to control.

(grain sizes ~2 μm) had a very low solubility (Wang et al., 2016). The studied MoS_2 particles have a specific surface area of 8.96 m^2/g, and the total surface area of the retained particles in the lung tissue was estimated to be 15.4 cm^2 at High exposure. Others have reported thresholds for neutrophil influx of 20 cm^2 for carbon black particles (Stoeger et al., 2006).

No histopathological effects were found in liver and kidney, suggesting that the amounts of molybdenum (disulphide) reaching these organs were not sufficient to induce detectable morphological signs of toxicity. Indeed, translocation from lung to systemic circulation is highly size-dependent (Stone et al., 2017). Notably, molybdenum translocates to kidneys after inhalation as seen in seven workers who accidentally

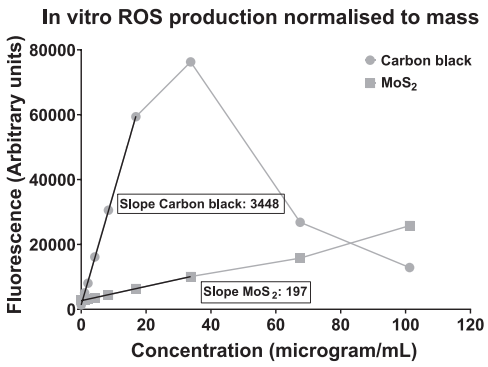

Fig. 5. ROS production from MoS_2 and Printex 90. Values are shown as mean arbitrary units of three replicates, within one experiment. Slopes for each concentration-response curve were calculated using linear regression, in the range of 0–16.9 μg/mL for Printex 90 and 0–33.8 μg/mL for MoS_2.

inhaled ^{99}Mo (Alvarez et al., 1994); and it was seen in urine at substantial levels in workers from a molybdenite roasting plant (Walravens et al., 1979). Moreover, ^{99}Mo was distributed to liver and kidney among other organs in dogs after inhalation (Cuddihy et al., 1969). Unfortunately, the studies did not provide information regarding particles size. In the present experimental setup, we were not able to assess lung histopathology, and thus we were not able to pathologically corroborate the finding of irritation in the plethysmograph study. However, the fact that no exposure-related effects on LDH and protein content in BALF were detected argues against exposure-related tissue damage. Histopathologic changes in the lungs were reported in the aforementioned chronic exposure study with MoO_3 in rodents already at 10 mg/m^3 (=8 mg Mo/m^3) (Chan, 1998; NTP, 1997).

4.4. Genotoxicity

Increased genotoxicity was seen for the Mid and High exposures in BAL fluid cells (Fig. 4). No increased genotoxic effect was seen lung and liver with the investigated time-period (Supplementary Materials Fig. S6). It is unknown whether a longer exposure duration or post-exposure duration would have shown another pattern of genotoxicity perhaps also occurring in lung and liver. Other assays e.g. micronuclei detection in erythrocytes or chromosomal aberrations in bone marrow cells could have been relevant assays for genotoxicity assessment. Yet the comet assay allows us to screen specific cells and tissues that are among the first to interact with the MoS_2 particles upon inhalation (BAL fluid cells, lung and liver tissue).

One in vitro study found no genotoxicity of MoS_2 neither in human kidney epithelial cells (HEK293f), nor in *Salmonella typhimurium* (Appel et al., 2016). Concerning other molybdenum substances, the NTP study mentioned in the introduction did not investigate genotoxicity, but rather the ultimate result of it, namely carcinogenicity. The authors of that study concluded the evidence for carcinogenicity of MoO_3 inhalation was equivocal in male rats, that there was no evidence in female rats, whereas there was some evidence for carcinogenicity in mice (Chan, 1998; NTP, 1997). Of note, MoS_2 and MoO_3 are different chemical compounds with different physico-chemical properties that may affect their toxicological properties, even though both contain molybdenum.

Concerning other molybdenum substances, molybdenum nanoparticles were genotoxic in vivo (Mohamed et al., 2020). Molybdenum (IV) sulphide nano- and microparticles were not genotoxic in vivo (Sobańska et al., 2020), while there were both a positive and a negative in vivo study on sodium molybdate (ECHA, 2020; Titenko-Holland et al., 1998). Concerning genotoxicity of other molybdenum substances determined in vitro, this metal appears to be negative, as multiple studies were negative, while only a few were positive (Hadrup et al., 2022).

Overall, our data suggested a genotoxic effect of MoS_2 in vivo. Although there are carcinogenicity data on MoO_3 and in vivo data on various molybdenum compounds, it is unknown whether the carcinogenicity and genotoxicity observed for those compounds are caused by their particular chemical composition, or by release of molybdenum. Thus, we suggest that future studies on MoS_2 are needed to corroborate that this substance is genotoxic following pulmonary exposure. In addition, the mechanism of action of the observed genotoxicity should be determined.

One question of interest in relation to a hazard assessment based on these genotoxicity results, is whether the effect is via a direct mechanism on the DNA (primary genotoxicity), or via an indirect mechanism (secondary genotoxicity). We observed increased inflammation at the High exposure, indicating that inflammation could be involved. Nevertheless, the absence of inflammation at Mid exposure points to genotoxicity occurring in the absence of inflammation at that exposure level. One mechanism that can play a role is ROS generation, which we consider to be part of primary mechanisms of genotoxicity. We produced data on ROS production in an acellular assay; and found that the MoS_2 powder produced little ROS in comparison with the bench-mark material, carbon black, when normalised to mass. However, we found similar ROS production potentials of the two materials when normalised to specific surface area (Supplemental Fig. S7). Thus, it is possible that the observed genotoxicity is caused by ROS. Similarly, carbon black is a strong generator of ROS and induces increased levels of DNA strand breaks in vivo in mice (Di Ianni et al., 2022). Taking into account that carbon black induces genotoxicity in rodents at mass concentrations comparable to the lowest mass concentration of MoS_2 in the current study, 13 mg MoS_2/m^3 (0.8 mg/m^3 for 8 h working days) (Gallagher et al., 2003; Jackson et al., 2012; Saber et al., 2005), we cannot rule out that MoS_2 has a genotoxic mechanism that involves ROS production. But, the genotoxicity may involve other mechanisms too, e.g. effects on enzymes or direct effects on DNA.

5. Conclusion

After inhalation of MoS_2 in mice, one activated endpoint was genotoxicity in BAL fluid cells. In vitro ROS production was substantially lower than for carbon black nanoparticles used as bench-mark when normalised to mass, but similar when normalised to the specific surface area. This suggests that a ROS contribution to the observed genotoxicity cannot be ruled out. A No-observed-adverse-effect concentration (NOAEC) can be set to 13 mg/m^3 for 30 min inhalation per day, corresponding to 0.8 mg/m^3 for 8 h working days. This is based on genotoxicity in BAL fluid cells at the two highest exposure levels, and a slight body weight decrease occurring already at Mid exposure (50 mg/m^3). Nonetheless, an effect on respiratory function (decreased tidal volume) was already seen at lowest exposure level, 13 mg MoS_2/m^3 (0.8 mg/m^3 for 8 h working days), suggesting that this level was a LOAEC.

CRediT authorship contribution statement

Jorid B. Sørli: Conceptualization, Investigation, Formal analysis, Visualization, Writing – review & editing, Funding acquisition; **Alexander C.Ø. Jensen:** Investigation, Formal analysis, Writing – review & editing. **Alicja Mortensen:** Investigation, Formal analysis, Visualization, Writing – review & editing. **Józef Szarek:** Investigation, Formal analysis, Visualization, Writing – review & editing. **Claudia A.T. Gutierrez:** Investigation, Formal analysis, Visualization, Writing – review & editing. **Lucas Givelet:** Investigation, Formal analysis, Writing – review & editing. **Katrin Loeschner:** Investigation, Formal analysis, Writing – review & editing. **Charis Loizides:** Investigation, Formal analysis, Writing – review & editing. **Iosif Hafez:** Investigation, Formal analysis, Writing – review & editing. **George Biskos:** Investigation, Formal analysis, Writing – review & editing. **Ulla Vogel:** Formal

analysis, Writing – review & editing, Funding acquisition. **Niels Hadrup:** Conceptualization, Investigation, Formal analysis, Visualization, Writing – original draft, Writing – review & editing, Project administration, Funding acquisition.

Declaration of Competing Interest

The authors declare the following financial interests/personal relationships which may be considered as potential competing interests: Niels Hadrup reports financial support was provided by The Danish Working Environment Research Fund. Ulla Vogel reports financial support was provided by The Danish Government.

Data availability

Data will be made available on request.

Acknowledgments

The excellent technical assistance of Eva Terrida, Michael Guldbrandsen, Noor Irmam, Anne Abildtrup, Yasmin Akhtar, Signe Hjortkær Nielsen and Bianca Xuan Nguyen Larsen is greatly appreciated. This work was financed by a grant from the Danish Working Environment Research Fund ('Sikker-Motor'; number: 29–2019-09) and FFIKA, Focused Research Effort on Chemicals in the Working Environment, from the Danish Government.

Appendix A. Supporting information

Supplementary data associated with this article can be found in the online version at doi:10.1016/j.tox.2023.153428.

References

Alvarez, A., Navarro, N., Salvador, S., 1994. Urinary excretion measurements after accidental inhalation of 99mTc and 99Mo. Radiat. Prot. Dosim. 51, 59–61. https://doi.org/10.1093/oxfordjournals.rpd.a082122.

Appel, J.H., Li, D.O., Podlevsky, J.D., Debnath, A., Green, A.A., Wang, Q.H., Chae, J., 2016. Low cytotoxicity and genotoxicity of two-dimensional MoS 2 and WS 2. ACS Biomater. Sci. Eng. 2, 361–367. https://doi.org/10.1021/acsbiomaterials.5b00467.

Asgharian, B., Price, O.T., Oldham, M., Chen, L.-C., Saunders, E.L., Gordon, T., Mikheev, V.B., Minard, K.R., Teeguarden, J.G., 2014. Computational modeling of nanoscale and microscale particle deposition, retention and dosimetry in the mouse respiratory tract. Inhal. Toxicol. 26, 829–842. https://doi.org/10.3109/08958378.2014.935535.

Bengtson, S., Kling, K., Madsen, A.M., Noergaard, A.W., Jacobsen, N.R., Clausen, P.A., Alonso, B., Pesquera, A., Zurutuza, A., Ramos, R., Okuno, H., Dijon, J., Wallin, H., Vogel, U., 2016. No cytotoxicity or genotoxicity of graphene and graphene oxide in murine lung epithelial FE1 cells in vitro. Environ. Mol. Mutagen. 57, 469–482.

Booth, A., Jensen, K., 2015. NANoREG D4.12 SOP Probe Sonicator Calibration for ecotoxicological testing.

Boyles, M., Murphy, F., Mueller, W., Wohlleben, W., Jacobsen, N.R., Braakhuis, H., Giusti, A., Stone, V., 2022. Development of a standard operating procedure for the DCFH 2 -DA acellular assessment of reactive oxygen species produced by nanomaterials. Toxicol. Mech. Methods 32, 439–452. https://doi.org/10.1080/15376516.2022.2029656.

Brand, P., Bauer, M., Gube, M., Lenz, K., Reisgen, U., Spiegel-Ciobanu, V.E., Kraus, T., 2014. Relationship between welding fume concentration and systemic inflammation after controlled exposure of human subjects with welding fumes from metal inert gas brazing of zinc-coated materials. J. Occup. Environ. Med 56, 1–5. https://doi.org/10.1097/JOM.0000000000000061.

Chan, P., 1998. Lung tumor induction by inhalation exposure to molybdenum trioxide in rats and mice. Toxicol. Sci. 45, 58–65. https://doi.org/10.1006/toxs.1998.2497.

Cosnier, F., Seidel, C., Valentino, S., Schmid, O., Bau, S., Vogel, U., Devoy, J., Gaté, L., 2021. Retained particle surface area dose drives inflammation in rat lungs following acute, subacute, and subchronic inhalation of nanomaterials. Part. Fibre Toxicol. 18, 29. https://doi.org/10.1186/s12989-021-00419-w.

Cuddihy, R., Boecker, B., Kanapilly, G., 1969. Tissue distribution of 99Mo in the beagle dog after inhalation of aerosols of various chemical forms. LF-41. Fission Prod. Inhal. Proj. 117–120.

Danielsen, P.H., Knudsen, K.B., Štrancar, J., Umek, P., Koklič, T., Garvas, M., Vanhala, E., Savukoski, S., Ding, Y., Madsen, A.M., Jacobsen, N.R., Weydahl, I.K., Berthing, T., Poulsen, S.S., Schmid, O., Wolff, H., Vogel, U., 2020. Effects of physicochemical properties of TiO2 nanomaterials for pulmonary inflammation, acute phase response and alveolar proteinosis in intratracheally exposed mice. Toxicol. Appl. Pharmacol. 386, 114830 https://doi.org/10.1016/j.taap.2019.114830.

Di Ianni, E., Jacobsen, N.R., Vogel, U.B., Møller, P., 2022. Systematic review on primary and secondary genotoxicity of carbon black nanoparticles in mammalian cells and animals. Mutat. Res. Mutat. Res. 790, 108441 https://doi.org/10.1016/j.mrrev.2022.108441.

Di Ianni, E., Møller, P., Mortensen, A., Szarek, J., Clausen, P.A., Saber, A.T., Vogel, U., Jacobsen, N.R., 2020. Organomodified nanoclays induce less inflammation, acute phase response, and genotoxicity than pristine nanoclays in mice lungs. Nanotoxicology 14, 869–892. https://doi.org/10.1080/17435390.2020.1771786.

ECHA, 2020. Resgistration Dossier: Distillates (petroleum), hydrotreated light, EC number: 265–149-8; CAS number: 64742–47-8.

Frazier, K.S., Seely, J.C., Hard, G.C., Betton, G., Burnett, R., Nakatsuji, S., Nishikawa, A., Durchfeld-Meyer, B., Bube, A., 2012. Proliferative and nonproliferative lesions of the rat and mouse urinary system. Toxicol. Pathol. 40, 14S–86S. https://doi.org/10.1177/0192623312438736.

Gallagher, J., Sams, R., Inmon, J., Gelein, R., Elder, A., Oberdorster, G., Prahalad, A.K., 2003. Formation of 8-oxo-7,8-dihydro-2′-deoxyguanosine in rat lung DNA following subchronic inhalation of carbon black. Toxicol. Appl. Pharmacol. 190, 224–231.

Hadrup, N., Aimonen, K., Ilves, M., Lindberg, H., Atluri, R., Sahlgren, N.M., Jacobsen, N. R., Barfod, K.K., Berthing, T., Lawlor, A., Norppa, H., Wolff, H., Jensen, K.A., Hougaard, K.S., Alenius, H., Catalan, J., Vogel, U., 2021. Pulmonary toxicity of synthetic amorphous silica - effects of porosity and copper oxide doping. Nanotoxicology 15, 96–113. https://doi.org/10.1080/17435390.2020.1842932.

Hadrup, N., Bengtson, S., Jacobsen, N.R., Jackson, P., Nocun, M., Saber, A.T., Jensen, K. A., Wallin, H., Vogel, U., 2017. Influence of dispersion medium on nanomaterial-induced pulmonary inflammation and DNA strand breaks: Investigation of carbon black, carbon nanotubes and three titanium dioxide nanoparticles. Mutagenesis 32. https://doi.org/10.1093/mutage/gex042.

Hadrup, N., Sørli, J.B., Sharma, A.K., 2022. Pulmonary toxicity, genotoxicity, and carcinogenicity evaluation of molybdenum, lithium, and tungsten: a review. Toxicology 467, 153098. https://doi.org/10.1016/j.tox.2022.153098.

Hahn, A., Burger, R., Begemann, K., 2012. Abstracts of the 2012 international congress of the european association of poisons centres and clinical toxicologists. Clin. Toxicol. 50, 273–366. https://doi.org/10.3109/15563650.2012.669957.

Harada, T., Enomoto, A., Boorman, G.A., Maronpot, R., 1999. Liver and gallbladder. In: Maronpot, R., Boorman, G.A., Gaul, B.W. (Eds.), Pathology of the Mouse. Cache River Press, pp. 119–183.

Haschek, W., Rousseaux, C., Wallig, M., 2010. Fundamentals of toxicologic pathology, 2nd ed..,. Elsevier Academic Press,.

Huber, E.A., Cerreta, J.M., 2022. Mechanisms of cell injury induced by inhaled molybdenum trioxide nanoparticles in Golden Syrian Hamsters, 153537022211040 Exp. Biol. Med. https://doi.org/10.1177/15353702221104033.

IPCS, 2004. IPCS Risk Assessment Terminology Part 1: IPCS/OECD Key Generic Terms used in Chemical Hazard/Risk Assessment Part 2: IPCS Glossary of Key Exposure Assessment Terminology.

Jackson, P., Hougaard, K.S., Boisen, A.M., Jacobsen, N.R., Jensen, K.A., Moller, P., Brunborg, G., Gutzkow, K.B., Andersen, O., Loft, S., Vogel, U., Wallin, H., 2012. Pulmonary exposure to carbon black by inhalation or instillation in pregnant mice: effects on liver DNA strand breaks in dams and offspring. Nanotoxicology 6, 486–500.

Jackson, P., Pedersen, L.M., Kyjovska, Z.O., Jacobsen, N.R., Saber, A.T., Hougaard, K.S., Vogel, U., Wallin, H., 2013. Validation of freezing tissues and cells for analysis of DNA strand break levels by comet assay. Mutagenesis 28, 699–707.

Jacobsen, N.R., Pojana, G., White, P., Moller, P., Cohn, C.A., Korsholm, K.S., Vogel, U., Marcomini, A., Loft, S., Wallin, H., 2008. Genotoxicity, cytotoxicity, and reactive oxygen species induced by single-walled carbon nanotubes and C(60) fullerenes in the FE1-Mutatrade markMouse lung epithelial cells. Environ. Mol. Mutagen. 49, 476–487.

Kyjovska, Z.O., Jacobsen, N.R., Saber, A.T., Bengtson, S., Jackson, P., Wallin, H., Vogel, U., 2015. DNA damage following pulmonary exposure by instillation to low doses of carbon black (Printex 90) nanoparticles in mice. Environ. Mol. Mutagen. 56, 41–49.

Mendel, R.R., Bittner, F., 2006. Cell biology of molybdenum. Biochim. Biophys. Acta - Mol. Cell Res 1763, 621–635. https://doi.org/10.1016/j.bbamcr.2006.03.013.

Modrzynska, J., Mortensen, A., Berthing, T., Ravn-Haren, G., Szarek, J., Saber, A.T., Vogel, U., 2021. Effect on mouse liver morphology of CeO2, TiO2 and carbon black nanoparticles translocated from lungs or deposited intravenously. Appl. Nano 2, 222–241. https://doi.org/10.3390/applnano2030016.

Mohamed, H.R., El-Atawy, R.H., Ghoneim, A.M., El-Ghor, A.A., 2020. Induction of fetal abnormalities and genotoxicity by molybdenum nanoparticles in pregnant female mice and fetuses. Environ. Sci. Pollut. Res. https://doi.org/10.1007/s11356-020-08137-0.

Nielsen, G.D., Larsen, S.T., Hougaard, K.S., Hammer, M., Wolkoff, P., Clausen, P.A., Wilkins, C.K., Alarie, Y., 2005. Mechanisms of acute inhalation effects of (+) and (-)-alpha-pinene in BALB/c mice. Basic Clin. Pharmacol. Toxicol. 96, 420–428. https://doi.org/10.1111/j.1742-7843.2005.pto_04.x.

NTP, 1997. NTP TECHNICAL REPORT ON THE TOXICOLOGY AND CARCINOGENESIS STUDIES OF MOLYBDENUM TRIOXIDE (CAS NO. 1313–27-5) IN F344/N RATS AND B6C3F MICE 1 (INHALATION STUDIES).

Ott, H., Prior, C., Herold, M., Riha, M., Laufer, G., Ott, G., 2004. Respiratory symptoms and bronchoalveolar lavage abnormalities in molybdenum exposed workers. Wien. Klin. Woche 116, 25–30.

Saber, A.T., Bornholdt, J., Dybdahl, M., Sharma, A.K., Loft, S., Vogel, U., Wallin, H., 2005. Tumor necrosis factor is not required for particle-induced genotoxicity and pulmonary inflammation. Arch. Toxicol. 79, 177–182.

Seely, J., 1999. Kidney. In Pathology of the Mouse. Cache River Press.

Sobańska, Z., Sitarek, K., Gromadzińska, J., Świercz, R., Szparaga, M., Domeradzka-Gajda, K., Kowalczyk, K., Zapór, L., Wąsowicz, W., Grobelny, J., Ranoszek-Soliwoda, K., Tomaszewska, E., Celichowski, G., Roszak, J., Stępnik, M., 2020. Assessment of acute toxicological effects of molybdenum(IV) disulfide nano- and microparticles after single intratracheal administration in rats. Sci. Total Environ. 742, 140545 https://doi.org/10.1016/j.scitotenv.2020.140545.

Sørli, J.B., Frederiksen, M., Nikolov, N.G., Wedebye, E.B., Hadrup, N., 2022. Identification of substances with a carcinogenic potential in spray-formulated engine/brake cleaners and lubricating products, available in the European Union (EU) - based on IARC and EU-harmonised classifications and QSAR predictions. Toxicology 477, 153261. https://doi.org/10.1016/j.tox.2022.153261.

Stoeger, T., Reinhard, C., Takenaka, S., Schroeppel, A., Karg, E., Ritter, B., Heyder, J., Schulz, H., 2006. Instillation of six different ultrafine carbon particles indicates a surface area threshold dose for acute lung inflammation in mice. Environ. Health Perspect. 114, 328–333. https://doi.org/10.1289/ehp.8266.

Stone, V., Miller, M.R., Clift, M.J.D., Elder, A., Mills, N.L., Møller, P., Schins, R.P.F., Vogel, U., Kreyling, W.G., Alstrup Jensen, K., Kuhlbusch, T.A.J., Schwarze, P.E., Hoet, P., Pietroiusti, A., De Vizcaya-Ruiz, A., Baeza-Squiban, A., Teixeira, J.P., Tran, C.L., Cassee, F.R., 2017. Nanomaterials versus ambient ultrafine particles: an opportunity to exchange toxicology knowledge. Environ. Health Perspect. 125, 106002 https://doi.org/10.1289/EHP424.

Thoolen, B., Maronpot, R.R., Harada, T., Nyska, A., Rousseaux, C., Nolte, T., Malarkey, D. E., Kaufmann, W., Küttler, K., Deschl, U., Nakae, D., Gregson, R., Vinlove, M.P., Brix, A.E., Singh, B., Belpoggi, F., Ward, J.M., 2010. Proliferative and Nonproliferative Lesions of the Rat and Mouse Hepatobiliary System. Toxicol. Pathol. 38, 5S–81S. https://doi.org/10.1177/0192623310386499.

Titenko-Holland, N., Shao, J., Zhang, L., Xi, L., Ngo, H., Shang, N., Smith, M.T., 1998. Studies on the genotoxicity of molybdenum salts in human cells in vitro and in mice in vivo. Environ. Mol. Mutagen. 32, 251–259. https://doi.org/10.1002/(SICI)1098-2280(1998)32:3<251::AID-EM8>3.0.CO;2-R.

Vijayaraghavan, R., Schaper, M., Thompson, R., Stock, M.F., Alarie, Y., 1993. Characteristic modifications of the breathing pattern of mice to evaluate the effects of airborne chemicals on the respiratory tract. Arch. Toxicol. 67, 478–490. https://doi.org/10.1007/BF01969919.

Vijayaraghavan, R., Schaper, M., Thompson, R., Stock, M.F., Boylstein, L.A., Luo, J.E., Alarie, Y., 1994. Computer assisted recognition and quantitation of the effects of airborne chemicals acting at different areas of the respiratory tract in mice. Arch. Toxicol. 68, 490–499. https://doi.org/10.1007/s002040050101.

Wang, Z., von dem Bussche, A., Qiu, Y., Valentin, T.M., Gion, K., Kane, A.B., Hurt, R.H., 2016. Chemical dissolution pathways of MoS 2 nanosheets in biological and environmental media. Environ. Sci. Technol. 50, 7208–7217. https://doi.org/10.1021/acs.est.6b01881.

Winer, W.O., 1967. Molybdenum disulfide as a lubricant: a review of the fundamental knowledge. Wear 10, 422–452. https://doi.org/10.1016/0043-1648(67)90187-1.